Higgs-boson production from decays of the fourth-generation b' quark

Wei-Shu Hou
Paul Scherrer Institute, CH-5232 Villigen PSI, Switzerland

Robin G. Stuart
Theory Division, CERN, CH-1211 Geneva 23, Switzerland
(Received 17 August 1990)

In a scenario in which the fourth-generation b' quark is lighter than m_t+M_W, flavor-changing neutral-current $b'\to b$ transitions could be substantial. In particular, the decay $b'\to bH$ could be dominant or comparable to the processes $b'\to ce\bar{\nu}$ and/or $b'\to bZ$ for a wide range of the parameters $m_{b'}$, m_t, $m_{t'}$, M_H, $V_{cb'}$, and $V_{tb'}$. For $b'\bar{b}'$ pairs the latter decays could provide valuable leptonic tags for Higgs-boson production that is especially useful in hadronic colliders for a Higgs boson in the intermediate-mass range $M_Z<M_H<2M_W$. If $b'\to b\gamma$ is observed then the strict limit $M_H>m_{b'}-m_b$ is implied for $m_{b'}<M_Z$. We study the singularities exhibited by the effective flavor-changing neutral-current vertex $b'bH$ and identify them as anomalous thresholds. Experimental prospects are discussed.

I. INTRODUCTION

To date two essential ingredients of the standard model of electroweak interactions remain undiscovered: the top quark and the Higgs particle. Whereas the discovery of the top would mark the natural completion of the first three families of the fermions, the only evidence for the Higgs boson remains theoretical.

Recent results from the CERN e^+e^- LEP collider (Ref. 1) seem to exclude a Higgs boson with a mass up to 40 GeV and all the way down to 0 GeV. Ultimately LEP II could probably push this limit up to M_Z by looking for the process $e^+e^-\to HZ$.[2] If it is not found at LEP then, at least in the short term, one will probably have to rely on hadronic colliders to continue the search for this elusive particle. Unfortunately, the region $M_Z\leq M_H\leq 2M_W$, often called the "intermediate-mass Higgs-boson," is rather difficult to explore[3] with hadronic machines because of the lack of suitable tags.

Following a suggestion by the authors,[4,5] searches have been made for the fourth-generation, charge $-\frac{1}{3}$ quark (b') with $m_{b'}<m_t$.[6-12] It was argued that, with reasonable assumptions on the structure of the 4×4 Kobayashi-Maskawa (KM) matrix, flavor-changing neutral-current (FCNC) processes $b'\to bg, b\gamma, bZ$ could be the dominant decay modes and that therefore the b' would evade discovery by searches based on the usual charged-current (CC) signature of "isolated e/μ+jets." Haeri, Soni, and Eilam[13] noted that, in this scenario, the decay $b'\to bH$ offers new possibilities for Higgs-boson search up to $M_H=m_{b'}-m_b$. Some insight can be gained simply by scaling up from the B system. For that reason it is useful to briefly review the situation there. Only charge $-\frac{1}{3}$ quarks provide suitable laboratories for Higgs-boson searches because their lifetimes are prolonged by small quark mixing angles, while, at the same time, the pattern of the KM matrix elements allows them to be very sensitive to heavy quarks through loop effects. The b quark is rather light but the Linde-Weinberg lower bound[14] on M_H is evaded if the top quark is heavy ($m_t\gtrsim M_W$). Assuming $m_t\sim M_W$, one finds[15] the branching ratio

$$B(b\to sH)\sim 0.3\left[1-\frac{M_H^2}{m_b^2}\right]^2\left|\frac{V_{ts}}{V_{cb}}\right|^2. \tag{1.1}$$

Since $V_{ts}\approx V_{cb}$, the decay $b\to sH$ yields very powerful limits whenever data are available with the only significant theoretical uncertainty being the top-quark mass. These limits are now superseded by direct limits from LEP.[1]

The branching ratio given by Eq. (1.1) is rather large (as compared to $b\to c$ transitions) and $b\to sH$ dominates over all other FCNC $b\to s$ processes, whenever kinematically allowed. Thus it is reasonable to expect that $b'\to bH$ could be comparable to or dominant over the FCNC modes of the b' when it is allowed kinematically. In addition, because of likely KM suppression in the CC decay $b'\to c$, it might also be comparable to or dominant over all other modes. If the $b'\to bH$ mode is substantial but not predominant, then decays of a $b'\bar{b}'$ pair in which one of the quarks decays producing a Higgs boson and the other decays producing an isolated charged lepton $l^\pm$ or a charged-lepton pair l^+l^- ($M_{ll}=M_Z$) could occur at a reasonable rate and would provide useful handles on Higgs-boson production. We have studied this possibility and presented a summary of our conclusions elsewhere.[16] It was found that this decay scenario may indeed facilitate Higgs-boson searches, particularly in the intermediate-mass region. Here we present a more detailed account and compare our results closely with those of other authors.

The decay process $b'\to bH$ has been studied by the present authors[16] and by Haeri, Soni, and Eilam.[13,17] (Reference 17 will henceforth be referred to as EHS.)

The work of Haeri, Soni, and Eilam, however, suffers from a number of inadequacies and limitations. These authors argued that the mode $b' \to bH$ will dominate over other FCNC $b' \to b$ processes when allowed kinematically, although they have not done a detailed calculation for $b' \to bZ$. They further concluded that if $m_{b'} < M_W$ and $M_H < 40$ GeV then $b' \to bH$ will dominate all modes including the CC decays $b' \to c$. It should be noted that if this were the case then in hadronic machines, neither the b' nor the Higgs boson would be easy to extract from the very severe QCD backgrounds. In actual fact the outlook may not be so bleak since EHS chose a very specific and restricted form of the 4×4 KM matrix in which $V_{tb'} \sim \theta^3$ and $V_{cb'} \sim \theta^4$ with $\theta \sim 0.22$, the Cabibbo angle. If the fourth generation exists it is probable that $V_{tb'}$ is not small compared to θ since m_t and $m_{t'}$ might be the most closely spaced masses for adjacent pairs of like-charged quarks. Judging from the observed pattern $V_{ub} \ll V_{cb} \ll V_{us}$ it may reasonably be expected that $V_{cb'} \ll V_{cb} \ll V_{tb'}$, with the last of these ($V_{tb'}$) being unsuppressed. The 4×4 KM matrix would then be roughly block diagonal. For the processes under consideration here note that $|V_{tb'}| \sim |V_{t'b} V_{t'b'}| \sim |V_{tb} V_{tb'}|$, provided $V_{tb'}$ is not much larger than the Cabibbo angle. The KM matrix elements can therefore be factored out in expressions for rates. It will be assumed here that the KM matrix elements are real since for our purposes *CP*-violating phases can be ignored.

EHS present their results by plotting the ratio of branching ratios:

$$R = \frac{\Gamma(b' \to bH)}{\Gamma(b' \to e\bar{\nu} + X)} , \tag{1.2}$$

with $\Gamma(b' \to e\bar{\nu} + X) \equiv \sum_{q=c,t} \Gamma(b' \to qe\bar{\nu}) \Theta(m_{b'} - m_q)$. Whereas this was a sensible choice for the B system it is not so here. In the B system, because of the smallness of V_{ub}, the analaogous ratio is quite insensitive to KM matrix elements. Both numerator and denominator depend essentially only on V_{cb} since $V_{cs}^* V_{cb} \approx -V_{ts}^* V_{tb} \approx V_{cb}$ which thus roughly cancels. The branching ratio $b \to e\bar{\nu} + X$ is well measured experimentally and therefore the branching ratio for $b \to sH$ can be deduced from a knowledge of R. The only m_b dependence is of the rather trivial kind shown in Eq. (1.1). For the b', things are quite different. First, the structure of the 4×4 KM matrix is unknown and R is dependent on its form. In particular, the numerator depends mainly on $V_{tb'}$ and is insensitive to $V_{cb'}$ whereas the denominator is sensitive to both. As mentioned previously, it was shown recently by the authors of the present paper that if $m_{b'} < m_t$ then the FCNC decay modes could dominate.[4,5] Thus the CC branching ratio would be heavily suppressed and in itself hard to measure and therefore not such a convenient normalization factor. The quantity R as defined in (1.2) is also affected by the thresholds $b' \to t$ and $b' \to c$ that serve only to complicate the presentation since they are not in themselves the object of interest here.

We shall make a detailed study of CC and FCNC b' decays in a very broad range of parameter space, with an eye towards discovering the Higgs boson through the decay $b' \to bH$. Some questions may arise in the mind of the reader: Is the existence of a fourth generation still a viable option? If yes, is it reasonable to have the Higgs boson lighter than b' at the same time? Let us try to address these questions before we go on. It has been widely accepted that the "neutrino counting"[18] done by SLAC Linear Collider (SLC) and LEP experiments implies that there exists only three fermion generations. If one shares such belief, the whole scenario discussed here can be just brushed aside as ruled out already. However, it should be emphasized that the SLC and LEP experiments count only the number of *light* neutrinos (or any "invisible," light, particle that couples to the Z boson). What *is* ruled out is the existence of a fourth, light, neutrino. If the fourth "neutrino" is actually *heavy*, the existing experiments only provide the limit $m_{\nu_\sigma} > M_Z/2$,[18] where σ and ν_σ stand for the fourth-generation charged and neutral leptons. In this sense, searching for FCNC b' decays at high-energy colliders can be viewed as rather interesting, not only because of its peculiar event signature, but because one would be discovering a "nonsequential" generation, where the neutrino sector deviates from existing patterns in the first three generations. This view is apparently shared by the same experiments that found conclusive evidence for only three light neutrinos, as they continued to search for b' after their "neutrino-counting" results.[6–12] The search program must continue. With the top quark itself already rather heavy, it lends some circumstantial "weight" to the notion of having a new generation of fermions where the "neutrino" is heavy. Once one is convinced that the b' has to be searched for (in particular, its FCNC decay modes), it should be kept in mind that the Higgs boson may well be lighter than b', since we have no theory that accounts for the Higgs-boson mass. This is more so if the b' is heavy, allowing more room for the $b' \to bH$ mode to occur. One should therefore be aware how the phenomenology may change when the Higgs boson can appear in b' decay final state, and be prepared to devise strategies to study the potential signals. As we shall see, in light of the Collider Detector at Fermilab limit of $m_t > 89$ GeV,[19] the intermediate-mass Higgs-boson region $M_Z \lesssim M_H \lesssim 2M_W$ could be covered if the b' is heavy enough, but not heavier than $m_t + M_W/2$.

The layout of this paper is as follows. In Sec. II we describe the details of our own calculation. In Sec. III we discuss the numerous checks that we have applied to our analytic results to ensure their correctness. Here it is noted that, for certain choices of the parameters, anomalous thresholds occur in the effective $b'bH$ FCNC vertex. We study these and suggest a physically motivated fix for them. In Sec. IV the numerical results and experimental prospects are discussed and our conclusions are summarized in Sec. V.

II. THE CALCULATION OF $\Gamma(b' \to BH)$

The general effective $b'bH$ vertex can be written in the form

$$\frac{g^3}{32\pi^2 M_W} V_{tb} V_{tb'} H\bar{b}(m_b h_L \gamma_L + m_{b'} h_R \gamma_R) b' , \tag{2.1}$$

where γ_L and γ_R are the left- and right-handed helicity projection operators, respectively. The KM matrix elements can be factorized since the effective coupling is sensitive only to heavy fermions, and because $V_{cb'} \ll V_{tb'}$ is assumed. Hence, the form factors satisfy $h_{L,R} \equiv h^t_{L,R} - h^{t'}_{L,R}$, where the superscripts denote the flavor of the internal quark appearing in the one-loop FCNC vertex diagrams. Note that only the h_R form factor contributes to the rate when $m_b = 0$.

The Feynman diagrams contributing to the general FCNC decay vertex QqH are shown in Fig. 1. In the case of interest here Q stands for the incoming heavy quark and q for the lighter outgoing quark. The internal virtual quark is denoted by i. We calculate in the 't Hooft–Feynman gauge (R_ξ gauge with $\xi = 1$). Diagrams containing virtual charged Goldstone scalars then contribute but the algebraic expressions for individual diagrams are considerably simpler than they would be if unitary gauge ($\xi = \infty$) were used. The authors have already undertaken an analogous calculation for the process $b' \to bV$ where $V = \gamma, g$ or Z^0.[4,5] The same number of Feynman diagrams have to be evaluated as in the present case but the additonal γ algebra complicates matters considerably. The general $b'bV$ vertex is of the form

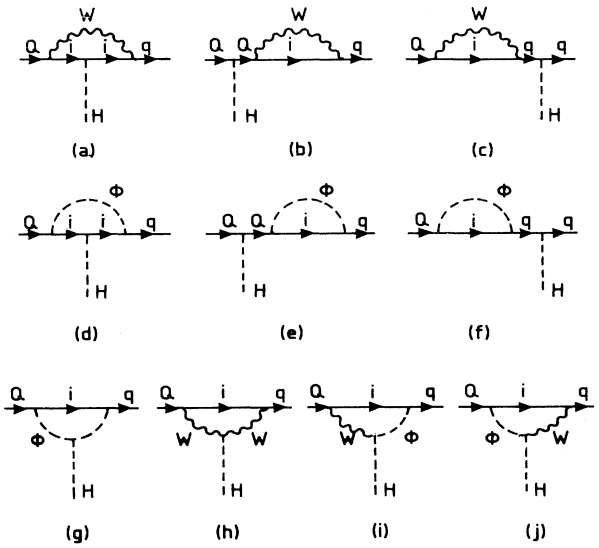

FIG. 1. Feynman diagrams contributing to the flavor-changing neutral-current Higgs vertex, QqH in 't Hooft–Feynman gauge (R_ξ gauge with $\xi = 1$). The internal quark is denoted by i.

$$\gamma_\mu(f_L\gamma_L + f_R\gamma_R) + i\sigma_{\mu\nu}q_\nu(f_{TL}\gamma_L + f_{TR}\gamma_R) + q_\mu(f_{LL}\gamma_L + f_{LR}\gamma_R) ,$$

which contains six form factors compared to two in the general $b'bH$ coupling. Here q_μ is the four-momentum of the vector boson.

The basic strategy of the calculation is that followed in Refs. 4, 5, and 20. The diagrams in Fig. 1 are calculated with general couplings and in terms of a standard set of integrals defined by Passarino and Veltman.[21] This step requires a minimum of hand calculation. The expressions are then separately coded in the algebraic-manipulation language REDUCE. With this code at our disposal it is a simple matter to calculate the FCNC effective vertex $ff'H$, where f and and f' are distinct fermion species, in any gauge theory simply by changing the couplings of individual diagrams appropriately. The expressions in terms of standard integrals are then reduced by the package LERG–I (Refs. 22 and 23) written by one of the authors, to a few simple scalar integrals B_0 and C_0 multiplied by rational functions of masses and momenta squared. This form has a number of advantages. The expressions thus obtained tend to be numerically more stable than the original expressions because most potential strong cancellations have been removed at the analytic level. In addition, the final form is unique which means that, when adopted, calculations by different groups can be compared easily and directly. This is not in general possible otherwise and, as we shall see later, has practical repercussions for the present calculation.

The scalar integrals B_0 and C_0 are defined in Appendix A.

REDUCE can produce its output as FORTRAN code and this feature is used to avoid copying errors that might occur in encoding expressions for numerical evaluation. Reliable numerical routines are available for the evaluation of B_0 and C_0 that are readily incorporated along with the REDUCE output.

Throughout this paper we use the Euclidean metric with timelike momenta squared being negative. Conversion between the two metrics is achieved by switching the sign of squared momenta. In cases where results are given in terms of masses only, no conversion is necessary.

The final expressions for h_L and h_R are considerably shorter than in the analogous case for vector bosons.[4,5] A further simplification is obtained by ignoring the b-quark mass as it is much smaller than $m_{b'}$ in the range considered here and also compared to M_W. In that case only h_R contributes and the complete, relatively compact, expression is given in Appendix A. We have checked that setting $m_b = 0$ makes no significant difference in the final results. The decay rate for $b' \to bH$ is, then,

$$\Gamma(b' \to bH) = \frac{g^2}{32\pi}\left[\frac{g^2}{32\pi^2}\right]^2 |V_{tb}V_{tb'}|^2 \left[1 - \frac{M_H^2 - m_b^2}{m_{b'}^2}\right] \frac{m_{b'}^3}{M_W^2} |h_R|^2 \frac{2|\mathbf{p}_H|}{m_{b'}} , \tag{2.2}$$

where $\mathbf{p}_H$ is the three-momentum of the Higgs boson and for numerical purposes m_b is kept in both the matrix element squared and in the phase space. Equation (2.2) yields the known result for $\Gamma(b\to sH)$ (Ref. 15) after taking the appropriate limits.

From simple crossing one arrives at the process $H\to b'\bar{b}$, and one could ask whether such a decay process may help in the search for Higgs bosons. It turns out that the decay rate $H\to b'\bar{b}$ is never more than a few percent of $H\to b\bar{b}$, and we relegate the discussion to Appendix B.

For the purposes of later comparison, we give the charged-current semileptonic decay rate,

$$\Gamma[b'\to(c,t)+e\bar{\nu}]/\Gamma_0=|V_{tb'}|^2\left[\left|\frac{V_{cb'}}{V_{tb'}}\right|^2 f(\rho,\mu_c,\gamma)+f(\rho,\mu_t,\gamma)\Theta(m_{b'}-m_t)\right], \tag{2.3}$$

where $\Gamma_0=G_F^2 m_{b'}^5/(192\pi^3)$, $\rho=m_{b'}^2/M_W^2$, $\mu_i=m_i^2/M_W^2$, $\gamma=\Gamma_W^2/M_W^2$, and[24]

$$f(\rho,\mu,\gamma)=2\int_0^{(1-\sqrt{\mu})^2}\frac{dx}{(1-\rho x)^2+\gamma}[(1-\mu)^2+(1+\mu)x-2x^2][1+\mu^2+x^2-2(\mu+\mu x+x)]^{1/2}, \tag{2.4}$$

which is valid whether the $e\bar{\nu}$ comes from real- or virtual-W-boson decays. Thus, Eq. (2.3) accounts for the CC semileptonic decay rate for arbitrary b' and t masses, and depends on the mixing angles $V_{cb'}$ and $V_{tb'}$. We shall assume that $m_{b'}<m_{t'}$, since otherwise the b' decay rate would not be KM suppressed, and FCNC decays become relatively uninteresting as a discovery mode.

III. CHECKS

Although the procedure for calculating loop-induced FCNC effective interactions are, in principle, quite straightforward, it is rather tedious and it is well known that such calculations are vulnerable to various numerical sensitivities. In this section we discuss various checks that were performed on our results. We also identify the emergence of anomalous thresholds, which is briefly discussed for sake of completeness.

A. Low-energy limit

With the general effective $b'bH$ vertex written in the form of Eq. (2.1) one can set the external fermion masses equal to zero to check for agreement with the known results valid for the decays $s\to dH$ and $b\to sH$:[15]

$$h_R^t-h_R^0=\frac{3}{4}\frac{m_t^2}{M_W^2}. \tag{3.1}$$

Using the results of Grądkowski and Krawczyk[25] this check can also be performed diagram by diagram. Our expressions reduce to the correct limits in both cases.

B. Ward identities

As stated earlier, we have calculated in a previous paper, the one-loop FCNC vertices, $b'b\gamma$, $b'bg$, and $b'bZ$. The results were then applied to the study of FCNC decays of the b' quark. The fact that the first two of these vertices and the $\sin^2\theta_W$ dependent part of the third are associated with conserved currents leads to a constraint on the six possible form factors that can contribute to a general fermion–vector-boson coupling. In practice the six form factors are calculated essentially independently and the relationship demanded by current conservation provides a quite severe test. This test was performed analytically again using the package LERG–I and the key is to reduce all integrals appearing in the form factors to expressions only in terms of the scalar integrals B_0, C_0, and D_0 by the methods of Refs. 21–23. As mentioned previously the expressions generated by this strategy are unique. The loop-induced FCNC Z^0 current J_μ^Z and the FCNC pseudoscalar density J_5^Z, which couples to the unphysical Goldstone scalar ϕ_Z associated with the Z^0, are related through the Ward identity,

$$\partial_\mu J_\mu^Z=iM_Z J_5^Z. \tag{3.2}$$

The current J_μ^Z was calculated in the course of the work of Refs. 4 and 5 and J_5^Z can be obtained merely by substituting the appropriate couplings in the REDUCE code, discussed above, that generates the expression for the FCNC vertex $b'bH$. It is to be emphasized that this gives an independent check of both the present calculation and that of Ref. 5. While this check is severe it is not all encompassing as the analogs of diagrams (g) and (h) of Fig. 1 are not present in the case of ϕ_Z.

C. Comparison with EHS

We have also compared our results with those of EHS as given in their Table I. As noted above, the reduction of one-loop calculations to expressions in terms of B_0 and C_0 has a number of advantages, among these the uniqueness of the final form. The expressions given by EHS are in terms of the "nonscalar" integrals B_1, C_{11}, and C_{12}, and their form depends sensitively on the order chosen for the six arguments of C_{11} and C_{12} and the two mass arguments of B_1. For example,

$$B_1(q^2;m_1,m_2^2)=-B_1(q^2;m_2^2,m_1^2)-B_0(q^2;m_2^2,m_1^2). \tag{3.3}$$

Thus the results of EHS will not, in general, be directly comparable with other calculations. We have therefore taken their expressions and coded them in a form that can be processed by LERG–I, taking into account their

conventions. Fortunately this is relatively straightforward, and we find that their calculation agrees with ours diagram by diagram.

We have also attempted to reproduce some of the plots given by EHS. Figures 5–7 of Ref. 17 are very striking. They show a very sharp peak for certain parameter values but are presented without comment. We also find the same singular behavior and have been able to identify it with an anomalous threshold. This anomalous threshold appears in the physical region and it should be treated with care.

D. Anomalous thresholds

Since the phenomenon of anomalous thresholds seems nowadays to be remarkably little known, we digress a little and give a brief discussion of some of their properties. A fuller discussion can be found in Refs. 26–28.

An anomalous threshold appears as singular behavior in a loop integral but is not associated with poles or the crossing of a cut. The two-point function $B_0(q^2;m_1^2,m_2^2)$ has its physical threshold at $q^2=-(m_1+m_2)^2$ and an anomalous threshold at $q^2=-(m_1-m_2)^2$ but the latter does not occur on the physical sheet.

A necessary condition for having an anomalous threshold in the scalar three-point function $C_0(p_1^2,p_2^2,p_5^2;m_1^2,m_2^2,m_3^2)$ is that the external momentum arguments p_1^2, p_2^2, p_5^2 and the internal masses m_1^2,m_2^2,m_3^2 are such that at least two of the three possible cuts of the corresponding Feynman diagram can produce physical on-shell particles. Specifically at least two of the following conditions must be satisfied:

$$p_1^2 \le -(m_1+m_2)^2, \quad p_2^2 \le -(m_2+m_3)^2 , \quad p_5^2 \le -(m_1+m_3)^2 . \tag{3.4}$$

An anomalous threshold would be observed in the nucleon electromagnetic form factor were nucleon decays not forbidden by baryonic charge conservation. They do, however, appear for deuterons and hyperons. The deuteron, because of its small binding energy, has an anomalous threshold in its electromagnetic form factor in the low-q^2 timelike region. In electromagnetic scattering processes the cross section rises for $q^2\to 0$ in the spacelike region because of the influence of the anomalous threshold lying nearby but in the unphysical timelike region.

't Hooft and Veltman[29] have studied the scalar integrals B_0 and C_0 and have given an expression for C_0 as a sum of three integrals of the form

$$I=\int_0^1 dx \frac{\ln(ax^2+bx+c-i\epsilon)-\ln(ad^2+bd+c-i\epsilon)}{x-d} . \tag{3.5}$$

The coefficients a, b, c, and d depend on p_1^2, p_2^2, p_5^2, m_1^2, m_2^2, m_3^2, and a is assumed real. For real masses and at least one nonspacelike external momentum in C_0,

$$I=\mathrm{Sp}\left[\frac{d}{d-x_1}\right]-\mathrm{Sp}\left[\frac{d-1}{d-x_1}\right] +\mathrm{Sp}\left[\frac{d}{d-x_2}\right]-\mathrm{Sp}\left[\frac{d-1}{d-x_2}\right] , \tag{3.6}$$

where x_1,x_2 are the roots of the argument of the first logarithm in Eq. (3.5) obtained taking due care to respect the $i\epsilon$ prescription. The vanishing of the argument of the second logarithm in Eq. (3.5) is interpreted as an anomalous threshold. The imaginary part of the integral then displays a logarithmic singularity and the real part has a discontinuity. There is, however, no pole or crossing associated with this behavior. The singularity is maximally $\ln\epsilon$ and the discontinuity arises when the argument of one of the logarithms moves rapidly around the cut.

Consider now the calculation of $b'\to bH$ and choose, as did EHS in their Figs. 6 and 7, masses (in units of GeV) $M_W=80$, $m_{b'}=200$. An anomalous threshold is encountered for the case of $M_H=160$. Taking $m_b=0$ without loss of generality, the formula of 't Hooft and Veltman for argument of the second logarithm in Eq. (3.5) can be applied to the function $C_0(-m_{b'}^2,0,-M_H^2;M_W^2,m_t^2,M_W^2)$ that occurs in diagrams (g)–(j) in Fig. 1, to obtain a quadratic equation for the value of m_t^2 at which an anomalous threshold can arise. The result is

$$M_H^2 m_t^4+M_H^2(M_H^2-2M_W^2-m_{b'}^2)m_t^2+M_W^2(M_W^2M_H^2-M_H^2m_{b'}^2+m_{b'}^4)=0 , \tag{3.7}$$

which has the general solution

$$m_t^2=\tfrac{1}{2}(2M_W^2-M_H^2+m_{b'}^2)\pm\tfrac{1}{2}(M_H^2-m_{b'}^2)\left[1-\frac{4M_W^2}{M_H^2}\right]^{1/2} . \tag{3.8}$$

For the particular set of integer masses given above, the only solution lying on the physical sheet is $m_t=20\sqrt{34}\approx 116.62$. As M_H increases, the value of m_t where the anomalous threshold occurs also increases until it coincides with the physical threshold at $m_t=120$. The corresponding root of Eq. (3.7) attains its maximum value there and as M_H increases further it moves off the physical sheet. The behavior with respect to $m_{b'}$ of the real and imaginary parts of $C_0(-m_{b'}^2,0,-M_H^2;M_W^2,m_t^2,M_W^2)$ are shown in Figs. 2(a) and 2(b) for illustrative choices of mass parameters. From these figures we clearly see the discontinuity of the real part and the singularity of the imaginary part discussed above. This phemomenon occurs for a rather small range of parameter space. We have illustrated it with two singular cases of $M_H=2M_W,2M_W+0.2$, while for the other case of $M_H=2M_W-0.1$, the anomalous threshold disappears from the physical sheet.

With such genuine singularities occurring in a one-loop graph one should be loath to trust the predictions of perturbation theory nearby. If one does insist on calculating in such a region of parameter space a physically motivated fix is to include a finite width in the propagator of internal particles $(q^2+M_W^2-i\epsilon)^{-1}\rightarrow(q^2+M_W^2-i\Gamma_W M_W)^{-1}$. This effectively sums a subset of higher-order Feynman diagrams thereby taming the divergence. The correct inclusion of the width at the numerical level requires that one keeps careful track of the full analytic structure of the B_0 and C_0 functions so that imaginary parts of masses (i.e., widths) are properly handled. This is discussed in Ref. 29 and the expressions given there for B_0 and C_0 are shown to exhibit the correct behavior for masses with a negative imaginary part. Nevertheless the implementation of these formulas at the numerical level is nontrivial. Figure 3 shows the same set of curves as Fig. 2 except that a constant width $\Gamma_W=2$ GeV is included in the internal W-boson propagator. The cure is dramatic. The three curves corresponding to $M_H=2M_W-0.1, 2M_W, 2M_W+0.2$ now roughly coalesce. Note that such a fix does not work for the deuteron electromagnetic form factor, because the nucleons in the loop are rather stable particles. Another difference that weakens the threat in case of the deuteron is that the anomalous threshold in its electromagnetic form factor lies in the unphysical region, whereas in our case, it appears in the physical region.

In Figs. 4–6(a) we display the results of our calculation in a form identical to Figs. 5–7, respectively, of EHS. The narrowness of the anomalous threshold peaks indicate that the numerics are well handled.

Figure 5 of EHS agrees closely in form with our own Fig. 4 but does not display the detailed structure of nearby physical and anomalous thresholds. Here the physical threshold appears as a kink on the low M_H side of the anomalous threshold. Although not shown as such here, the spike of the anomalous threshold rises to infinity.

In our Figs. 5 and 6(a) the physical threshold appears as a kink on the right-hand side of the slope of the singularity, and exhibits rather intricate behavior with a minimum between the physical and anomalous thresh-

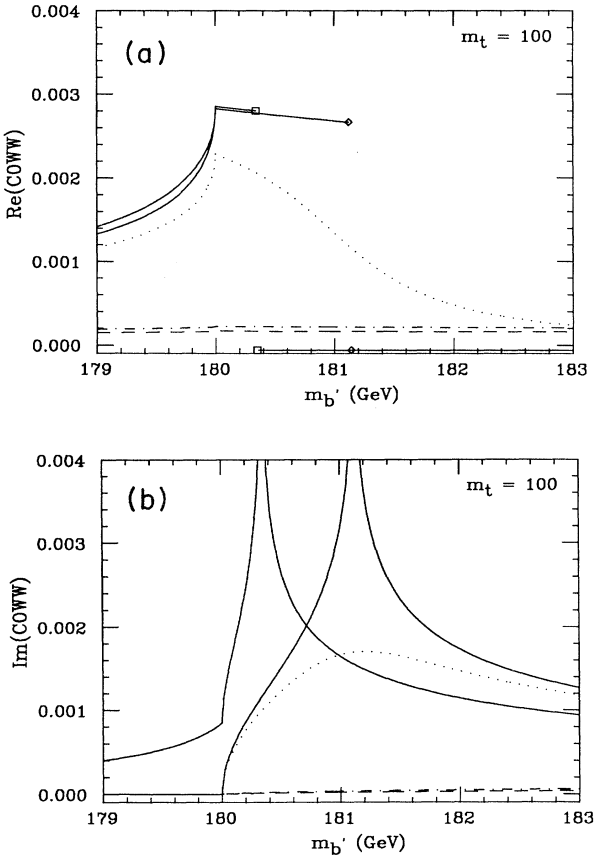

FIG. 2. The (a) real and (b) imaginary parts of the function $COWW\equiv C_0(-m_{b'}^2,0,-M_H^2;M_W^2,m_t^2,M_W^2)$ with $M_W=80$ GeV, $m_{b'}=100$ GeV, and $M_H=10$ (dashed), 100 (dot-dashed), 159.9 (dots), 160, i.e., $2M_W$ (solid, with diamond marker), 160.2 (solid, with square marker) GeV. For the last two M_W values, the real part exhibits a discontinuity (where we have attached the markers) and the imaginary part has a singularity at the anomalous threshold.

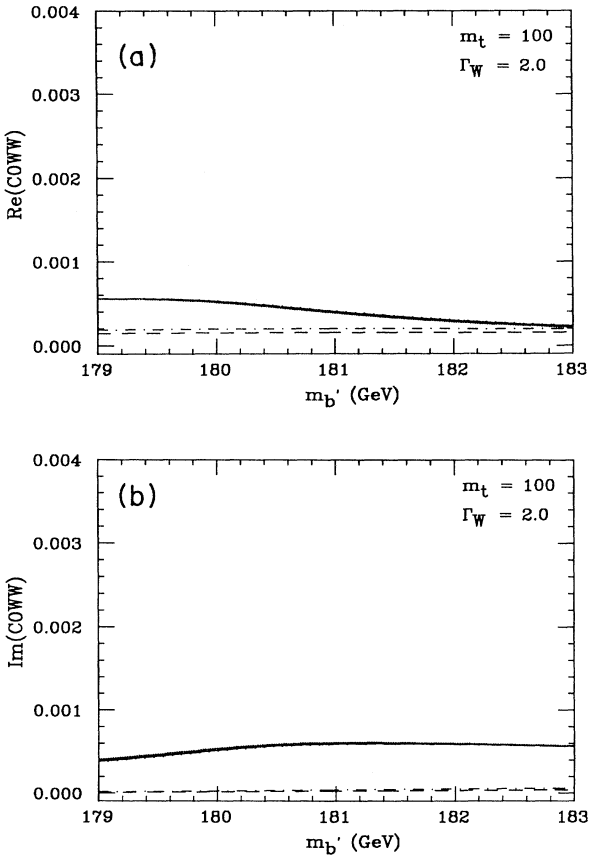

FIG. 3. As for Fig. 2 but including a $\Gamma_W=2$-GeV constant width in the W boson propagator. Note that the last three curves (with $M_H\approx 2M_W$) are no longer distinguishable.

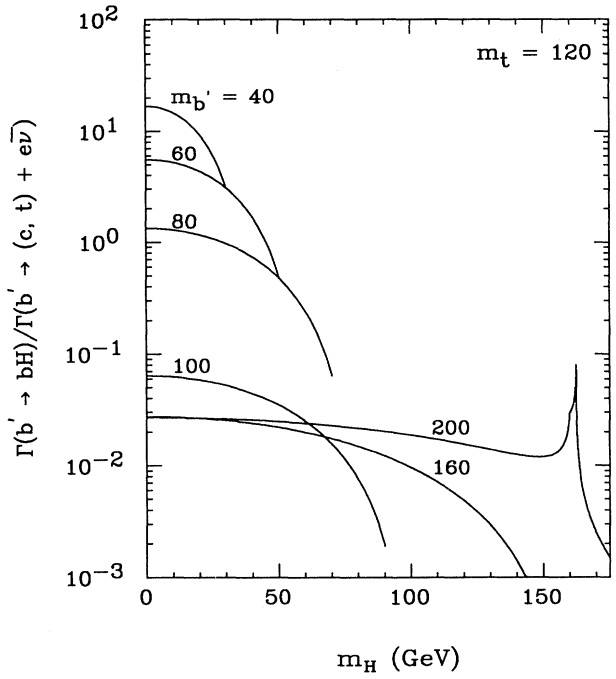

FIG. 4. The ratio $R \equiv \Gamma(b' \to bH)/\Gamma[b' \to (c,t) + e\bar{\nu}]$ plotted as a function of M_H for various values of $m_{b'}$ and $m_t = 120$ GeV, $m_{t'} = 250$ GeV corresponding to Fig. 5 of Ref. 17 and conventions defined therein.

olds. The dotted curves in these figures display the case for $M_H = 159.9$ GeV, that represent a tiny shift in M_H. The anomalous threshold has now left the physical sheet and the singularity is absent, although its effects can still be seen. The physical threshold is still apparent.

Figures 6 and 7 of EHS do not have this detailed structure. For their Fig. 7, a single peak is shown at the physical threshold $m_t = 120$ GeV rather than at the anomalous threshold, $m_t \approx 116.62$ GeV, which is in marked contrast to and inconsistent with their Fig. 6 in which the single peak appears at the anomalous threshold, but shows no evidence of the physical threshold.

Our Fig. 6(b) is the same as Fig. 6(a) except that a constant width of $\Gamma_W = 2$ GeV has been included in internal W boson propagators. The singularity is then removed and the dominant behavior near the anomalous threshold is governed by $\ln\Gamma_W$. Note that this procedure is not strictly equivalent to just including a finite width in the W mass where it appears as an argument of the C_0 form factor. The width must be included in the W propagator at the outset and carried consistently through the reduction process to scalar integrals, otherwise spurious behavior is generated in certain regions. The overall curve away from the anomalous threshold is rather insensitive to the presence of the finite width.

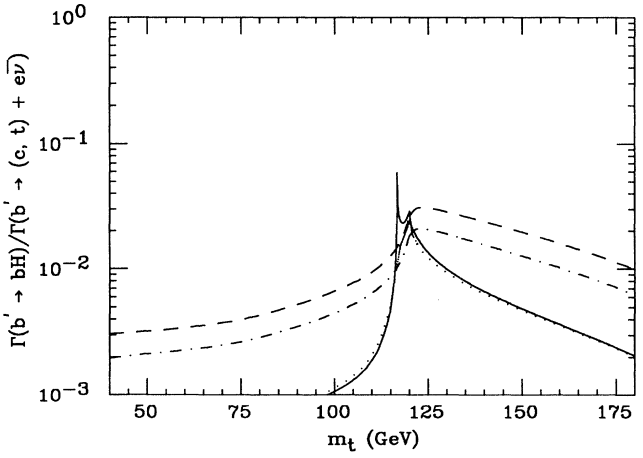

FIG. 5. The ratio R plotted as a function of m_t for (top to bottom) $M_H = 10$, 100, and 160 GeV and with $m_{b'} = 200$ GeV, $m_{t'} = 250$ GeV, corresponding to Fig. 6 of Ref. 17 and conventions defined therein. The dotted curve has $M_H = 159.9$ GeV for which the anomalous threshold lies just off the physical sheet.

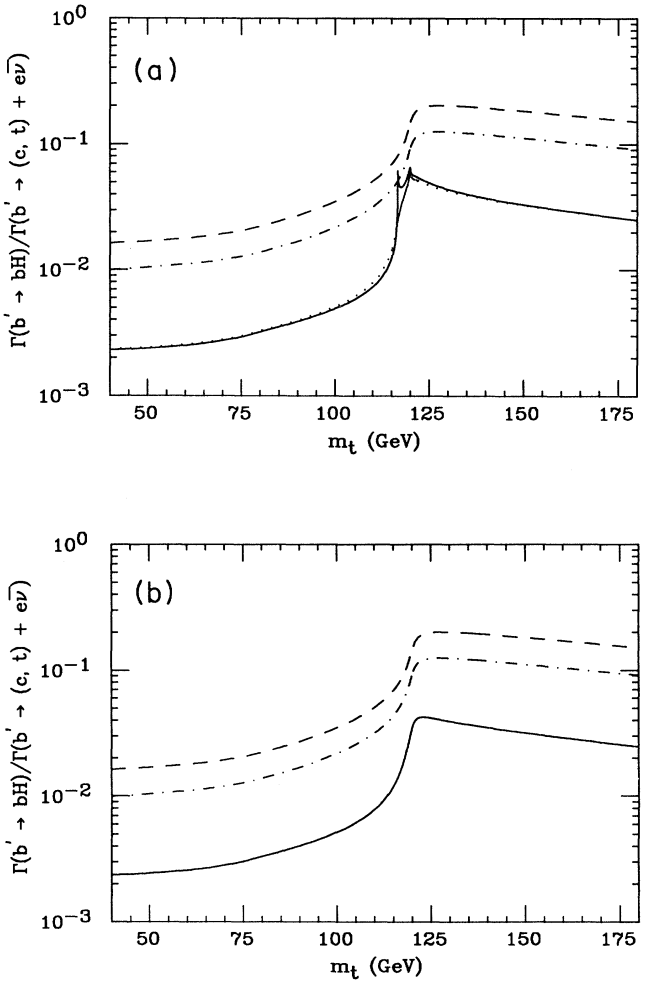

FIG. 6. As for Fig. 5 but with $m_{t'} = 400$ GeV, i.e, corresponding to Fig. 7 of Ref. 17, with (a) no width and (b) a constant width, $\Gamma_W = 2$ GeV, included in the internal W boson propagator.

E. Numerical evaluation

As explained above, our results satisfy the Ward identity (3.2). They also agree in the low-energy limit with Grządkowski and Krawczyk[25] and with Table I of EHS, diagram by diagram in both cases. These checks are performed by the algebraic-manipulation language REDUCE. We have checked, with the kind cooperation of Eilam, that the B_0's and C_0's of EHS agree numerically with ours to high precision. The largest discrepancy is of order 3% for $C_0(-m_{b'}^2,-m_b^2,-M_H^2;M_W^2,m_t^2,M_W^2)$ in the region very close to the anomalous threshold. In comparing B_0's since these functions are divergent, one has to, in practice, compute differences between pairs of B_0's. Our numerical B_0 and C_0 functions have also been subjected to other checks in the course of the analysis described in Refs. 4 and 5 and elsewhere.

The results of the EHS calculation initially disagreed with those presented here, the discrepancy being traced to those authors' encoding of their Table I for numerical evaluation. Our calculation is immune from errors of this kind as we generate a FORTRAN code directly from the same REDUCE source that has been shown to satisfy the several stringent tests described above. The problems encountered by EHS would have been largely avoided by using LERG−I.

IV. RESULTS AND PROSPECTS

A. Numerical results

Using Eq. (2.3), it can be shown that the charged-current decay rate $\Gamma[b'\to(c,t)+W^{(*)}]\cong 9\Gamma[b'\to(c,t)+e\bar{\nu}]$. This decay rate is shown in Fig. 7 for several values of m_t, as indicated, and for $m_{t'}=250$ GeV.[30] The decay rate includes both off- and on-shell W effects, where the factor of 9 is roughly accounted for by the decays $W^{(*)}\to e\bar{\nu}_e,\mu\bar{\nu}_\mu,\tau\bar{\nu}_\tau,\bar{u}d,\bar{c}s$. We have discarded $W^{(*)}\to\bar{t}b$ in the total CC b' decay rate since m_t is rather heavy in our applications, and the effect of this channel is heavily suppressed by phase space. Curves are plotted for the ratio $V_{cb'}/V_{tb'}=1$, 10^{-1}, 10^{-2}, and 10^{-3}. A factor $|V_{tb'}|^2$ has been removed from the decay rate to reduce dependence on unknown KM matrix elements and to make these plots more readily comparable with those of the FCNC decay modes $b'\to bH$ and $b'\to bZ$ given below. The sets of curves each show rapid upturns at the thresholds, $b'\to cW$, $b'\to tW^*$ [where the W is off shell but the Θ function in Eq. (2.3) is operative], and $b'\to tW$ (where both the t quark and W boson are on shell). Figure 8 is the same as Fig. 7 except that $m_{t'}=350$ GeV,[30] and the $m_{b'}$ interval has consequently been shifted upwards by 50 GeV. Because of the various thresholds, and because the controlling KM elements $V_{cb'}$, and $V_{tb'}$ would probably exhibit a strong hierarchy, one finds that the charged-current-induced b' decay rate could potentially be very suppressed, particularly for low $m_{b'}$. This region of prolonged b' lifetime expands as m_t is raised.

The possible b' lifetime could fall anywhere within a range that spans 10 orders of magnitude. This is a manifestation of the underlying condition that allows FCNC processes to be of importance for b' decays. Putting aside, for the moment, the possibility of the $b'\to bH$ decay, the authors have argued previously[4,5] that FCNC $b'\to b$ decays may well be the dominant b' decay modes, if $m_{b'}\lesssim m_t$ and if $V_{cb'}/W_{tb'}\lesssim 10^{-2}$. Below the $b'\to bZ$ threshold, the dominant FCNC decay modes would be $b'\to b\gamma$ (of order 10%), $b'\to bg$ (of order 45%), $b'\to bZ^*$ (of order 45%) (Ref. 31), while for $m_{b'}\gtrsim M_Z+m_b, b'\to bZ$ turns on and dominates the FCNC rate. The prospect of FCNC decay dominance changes the search strategy for b'considerably, and has influenced the experimenters at KEK TRISTAN, SLC, and LEP in their search for b', resulting,[6–12] in the current limit of $m_{b'}>M_Z/2$. The quest continues.

The possibility of having the Higgs boson light enough to be amongst the b' decay products complicates, but also further enriches, the potential phenomenology of the b'

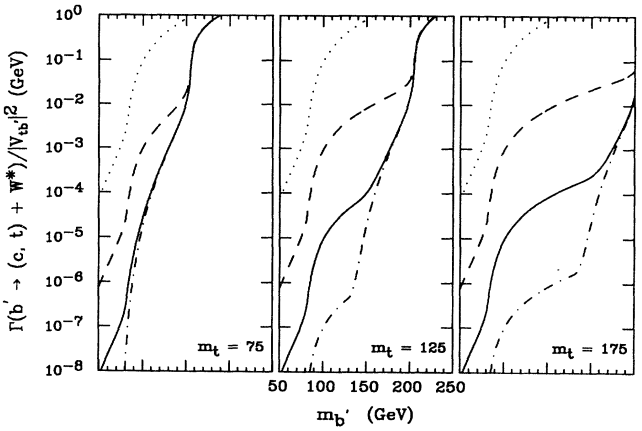

FIG. 7. Partial widths for charged-current decay $b'\to(c,t)+W^{(*)}$ plotted as a function of $m_{b'}$ for $m_{t'}=250$ GeV and m_t as indicated. The ratio $V_{cb'}/V_{tb'}$ is taken to be 1 (dotted), 10^{-1} (dashed), 10^{-2} (solid), and 10^{-3} (dot-dashed). The KM coefficient $|V_{tb'}|^2$ has been factored out.

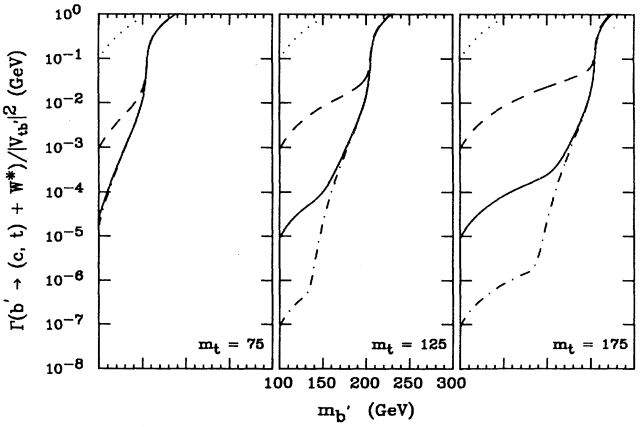

FIG. 8. As for Fig. 7, but $m_{t'}=350$ GeV.

quark. In particular, one may be hopeful that a new hunting ground for the Higgs particle could become available. In Fig. 9 we plot our results for the decay modes $b' \to bH$ and $b' \to bZ$ for $m_{t'} = 250$ GeV, in a similar framework as the CC decay result plotted in Fig. 7. The FCNC rates do not depend on $V_{cb'}$ as long as it is small compared to $V_{tb'}$, and the overall KM factor $|V_{tb}V_{tb'}|^2 \simeq |V_{tb'}|^2$ is taken out. The $b' \to bH$ rate, of course, depends on M_H, and we have illustrated for $M_H = 20$, M_Z, 150 and 200 GeV. Given the current lower bound on M_H from LEP, the first ($M_H = 20$ GeV) curve also serves the function of an upper limit for $b' \to bH$, which of course depends on the particular m_t and $m_{t'}$ values used. Similarly, for $m_{t'} = 350$ GeV, the FCNC decay results are given in Fig. 10, which should be compared to the CC decay result in Fig. 8. We have not placed emphasis here on the rather dramatic m_i^4 dependence on internal heavy-quark masses of the FCNC $b' \to bH$ and $b' \to bZ$ decay rates. Rather, we exhibit the $m_{b'}$ dependence, now including threshold effects, since this is of more relevance. The results are given for $m_{b'}$ almost up to $m_{t'}$. Once $m_{b'}$ rises above $m_{t'}$, the FCNC rates start to drop, while the CC $b' \to t, t'$ rates are at full strength and the FCNC decay scenario becomes uninteresting. Regions of parameter space in which anomalous thresholds occur have been avoided in these plots.

Let us now compare the results for CC and FCNC b' decays. There are basically four different mass regions of $m_{b'}$ that exhibit rather different decay properties. The boundaries of the regions are roughly defined by M_Z, $m_t + M_W/2$, and $m_t + M_W$.

At low b' masses ($M_Z/2 \lesssim m_{b'} \lesssim M_Z$), the $b' \to bZ$ curve can be matched smoothly onto $b' \to bZ^*$ by taking into account the finite Z^0 width, as well as box-diagram contributions.[31] By comparing with our earlier results,[4,5] one finds that $b' \to bH$ dominates the FCNC $b' \to b$ rate as long as it is kinematically allowed. Indeed, it may well dominate over $b' \to cW^{(*)}$ as long as $V_{cb'}/V_{tb'}$ is not much greater than $\sim 10^{-1}$, which was the main point emphasized by Haeri, Soni, and Eilam in Ref. 13, but was only illustrated with a particular choice of the 4×4 KM matrix. In the case where $b' \to bH$ is the predominant b' decay mode, the discovery of both b' and especially the Higgs boson in this process would become rather difficult. In hadronic machines, the $\bar{b}'b'$ pair produced via gluon fusion, subsequently decays into $\bar{b}Hb H$, with the Higgs boson decaying through $H \to \bar{b}b$. Thus, one has events with six b jets. Tagging the b's would not be particularly useful, but given the large hadronic production cross section, perhaps there are better hopes to use standard rare Higgs-boson decay mode techniques[3] to sift out the Higgs-boson production signal by exploiting the b' decay. If the $b' \to c$ transition is comparable to $b' \to bH$, then the real or virtual W decay can be used as a tag to enhance the chances of seeing a Higgs-boson signal. Even in the worst-case scenario, one is reminded that in this Higgs-boson and b' mass region one should be able to independently discover the Higgs boson and also identify the crossing of a new heavy flavor threshold at LEP II using event shape analysis or other means. Once the Higgs-boson mass and the crossing of a new flavor threshold are established, one should be able to work out the existence of the $b' \to bH$ mode in the LEP II environment, and perhaps in hadronic machines as well.

As M_H becomes heavier, the $b' \to bH$ mode freezes out. It does not have a "long tail" as in the Z^0-boson case since for this mass range the Higgs-boson width is very narrow due to its small Yukawa couplings to light final-state fermions. Once the $b' \to bH$ mode freezes-out, one is back in the scenario advocated by the authors,[4,5] that FCNC $b' \to b$ decays would dominate over CC $b' \to c$ decays, if $m_{b'} \lesssim m_t$ and $V_{cb'}/V_{tb'} \lesssim 10^{-2}$. This region extends from the far lower left corner of, for example, Figs. 7 and 9 and is not plotted. Further discussion can be found in Ref. 31. However, a rather interesting observation can be made here. Given that $b' \to bH$ would dominate $b' \to b$ transitions if it were allowed, the mere observation of $b' \to b\gamma$, $b' \to bg$ or $b' \to bZ^*$ decay modes

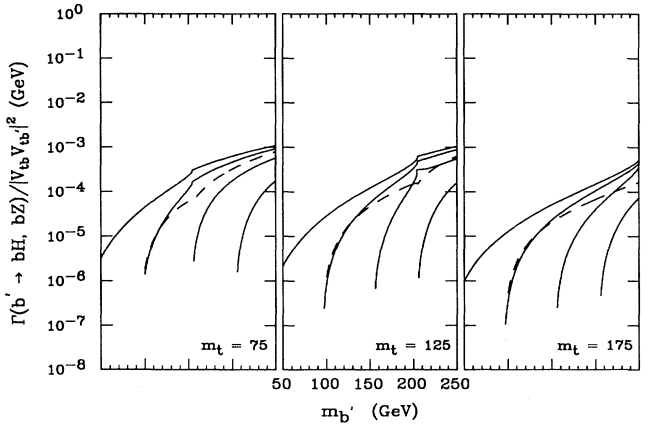

FIG. 9. Partial widths for the decay $b' \to bH$ as a function of $m_{b'}$ for $m_{t'} = 250$ GeV and Higgs-boson mass values (left to right) $M_H = 20$, M_Z, 150, 200 GeV. The dashed curve represents $\Gamma(b' \to bZ)$ with same set of parameters. The KM coefficient $|V_{tb'}V_{tb}|^2$ has been factored out.

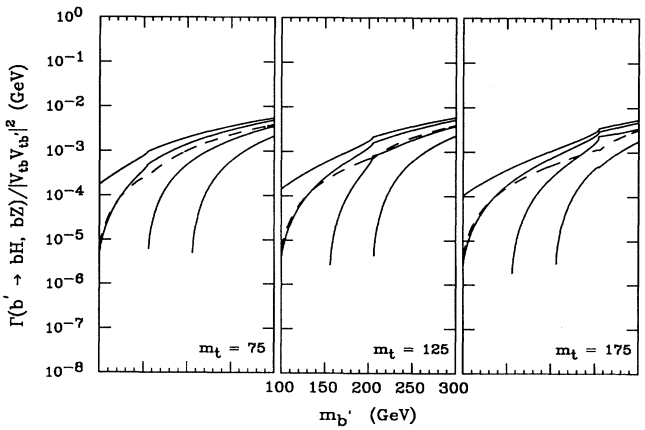

FIG. 10. As for Fig. 8 but $m_{t'} = 350$ GeV.

would rule out the Higgs boson up to $m_{b'}-m_b$. This powerful corollary is complementary to the standard Higgs-boson search strategy at e^+e^- colliders. In fact, first indications may well come from hadronic colliders given that the neutral-current signature $b'\to b\gamma$ probably could be managed in a hadronic environment.

As $m_{b'}$ moves above M_Z, the $b'\to bZ$ mode starts to turn on and dominates over the other gauge-boson-induced FCNC $b'\to b$ modes. The results, plotted as dashed lines in Figs. 9 and 10, can be easily compared with the $b'\to bH$ mode. It is readily seen that the two modes are quite comparable if $M_H\approx M_Z$. For lighter M_H, the Higgs mode definitely dominates $b'\to b$, but for heavier M_H, the Z^0 mode tends to dominate. The fact that $\Gamma(b'\to bH)\approx\Gamma(b'\to bZ)$ when $M_H\approx M_Z$ can be understood from the Ward identity (3.2). The "longitudinal" component of the Z^0 boson corresponds to the absorbed would-be neutral pseudoscalar Goldstone boson (ϕ_Z) originating from the same Higgs-boson doublet within the standard model, as embodied in (3.2). Thus it is no surprise that $b'\to bZ$ and $b'\to bH$ should have similar rates if the Higgs boson has a similar mass as the Z^0 boson. They share the strong dependence on internal quark masses since the Higgs sector generates both the symmetry breaking and the Yukawa coupling that leads to fermion masses.

Once $b'\to bZ$ turns on, so long as $b'\to bH$ is not strongly suppressed or forbidden by kinematics, the two rates never differ from each other by more than a factor of 10. This should provide an extra handle for the search of the Higgs boson in b' decay final state.

In the mass region $M_Z\lesssim m_{b'}\lesssim m_t+M_W/2$, comparing CC to FCNC b' decays, one observes the following. Let us define $r\equiv V_{cb'}/V_{tb'}$. For $r\gtrsim 5\times10^{-1}$, but depending somewhat on $m_{t'}$, $b'\to cW$ dominates although $b'\to bZ$ and $b'\to bH$ may still have some non-negligible branching ratios. For $10^{-2}\lesssim r\lesssim 5\times10^{-1}$, $b'\to cW$ and $b'\to b$ are comparable; for $r\lesssim 10^{-2}$, $b'\to b$ is dominant over $b'\to cW$, tW^*.[32] Thus, in general, this region has rather rich b' decay phenomenology.

In the mass region $m_t+M_W/2\lesssim m_{b'}\lesssim m_t+M_W$, the $b'\to tW^*$ rate turns on rapidly, and even if r is small enough to suppress the $b'\to cW$ rate, the overall CC decay rate is not small. Still, as long as r is not much larger than 10^{-2}, the FCNC $b'\to b$ decay may still have a branching ratio of 10% or more.

As $m_{b'}$ goes above the tW threshold, there are two qualitative changes. The CC decay $b'\to tW$ turns on, with a rate approaching 1 GeV (mod $|V_{tb'}|^2$). On the other hand, the $b'\to b$ decays are bounded above from the $M_H=20$-GeV curve, the dependence of which on $m_{b'}$ becomes softer, and never reaches much beyond 1 MeV (mod$|V_{tb}V_{tb'}|^2$). These two effects combine to make $\Gamma(b'\to tW)\gg\Gamma(b'\to b)$, independent of $V_{cb'}$, or equivalently r, and the FCNC $b'\to b$ modes become rare decays, as is normal, with branching ratios below $10^{-2}-10^{-3}$, depending on $m_{b'}$, m_t, and $m_{t'}$.

B. Physics prospects

The emerging picture should now be clear. If $m_{b'}\gtrsim m_t+M_W$, one has the usual CC predominance signature, and finding FCNC $b'\to b$ decays would be difficult, in particular, the isolation of Higgs bosons being produced in b' decay. If $m_{b'}\lesssim M_Z$, $b'\to bH$ would be predominant if it is kinematically allowed, and if $V_{cb'}/V_{tb'}$ is not too large. This situation would not be useful for discovery of the Higgs boson. Fortunately, one can discover the Higgs boson in such a mass range by rather conventional means, and the $b'\to bH$ decay would then serve as a confirmation of the overall picture that b' exists, and decays via a Higgs-boson-induced FCNC process. Implications can then be drawn on heavy fermion masses and $V_{cb'}/V_{tb'}$ when things become well understood. On the other extreme, there is the corollary that if $b'\to b\gamma$ or $b'\to bg$ or $b'\to bZ^*$ is observed, then the conclusion $M_H>m_{b'}-m_b$ can be drawn immediately, and much can be learned from a detailed study of the FCNC b' decay phenomenology. Of course, in between, the CC $b'\to c$ decay may also be present, which could serve as a tag.

For the intermediate region $M_Z\lesssim m_{b'}\lesssim m_t+M_W$ the possibilities are rich, but can be summarized in the following way: the three channels $b'\to bH$, $b'\to bZ$, and $b'\to cW$ (or $b'\to tW^*$) may all be comparable to one another, and they rarely differ by more than a factor of 10, unless $V_{cb'}/V_{tb'}$ is much greater than 10^{-1}, or if one is approaching the m_t+M_W threshold. Two explicit but general examples may serve to clarify the point.

Given the usual neutral-current constraints on mass splittings between quark doublet members, we consider the situation in which $m_{b'}$ is lower but not very different from $m_{t'}$. The first example we give, that satisfies all present constraints, is $m_{b'}=200$ GeV, $m_{t'}=250$ GeV, $m_t=175$ GeV, and $M_H=150$ GeV, with $V_{cb'}/V_{tb'}=10^{-2}$. Then, modulo $|V_{tb'}|^2$, one can read from Figs. 9 and 7 that the total width $\Gamma_{\rm tot}\simeq\Gamma(b'\to(c,t)+W^{(*)})+\Gamma(b'\to bH)+\Gamma(b'\to bZ)$ is roughly 4×10^{-4} GeV, with branching ratios, in order given above, of 62%, 14%, 24%, respectively. Thus, the FCNC decay branching ratios are quite sizable. Of course, as $V_{cb'}/V_{tb'}$ increases, the FCNC branching ratio decreases, but this could be compensated for by a lighter Higgs-boson mass. As a second example we consider $m_{b'}=150$ GeV, $m_{t'}=250$ GeV, $m_t=125$ GeV, and $M_H\cong M_Z$ with the same $V_{cb'}/V_{tb'}$. This situation may be an indication for supersymmetry[33] Then one finds $\Gamma_{\rm tot}\simeq 3\times10^{-4}$ GeV, where the three branching ratios are close to one another, each holding roughly $\frac{1}{3}$. It is clear that in both cases, there should be no problem in using either the Z^0, that must be on shell, or the W, that could also be virtual, as a tag for the b'-pair production events, and one could thereby have a rather enriched data sample that has a Higgs boson buried in it. With a change of parameters, one could encounter situations where only Z^0 or W serves as a tag, but not both. Note from these examples that all the "heavy" fermions (t, b', and t'), as well as the Higgs boson, have masses of order the weak symmetry-breaking scale. If that is the case, not only would there still be interesting phenomenology, as argued here, but one can ponder on its meaning as well.

The point to be emphasized is that, given the Collider

Detector at Fermilab limit of $m_t > 89$ GeV (Ref. 19), the mass range $M_Z \lesssim m_{b'} \lesssim m_t + M_W$ certainly allows the so-called intermediate-mass Higgs region $M_Z \lesssim M_H \lesssim 2M_W$ to be covered. In this case, one would actually prefer a heavier $m_{b'}$ to allow a more complete coverage, as illustrated by our first example above, provided that $m_{b'}$ does not exceed $m_t + m_W$. Thus, if the scenario is satisfied, a lot of work could be done at hadronic colliders, starting with the Fermilab Tevatron, and all the way to the CERN Large Hadron Collider (LHC) and the Superconducting Super Collider (SSC).

The potential signatures, and therefore the search strategies, are quite clear. Since for an e^+e^- machine, be it LEP or future multihundred GeV linear colliders, there are better signatures available, we therefore have in mind hadronic machines, from the currently running CERN ACOL or the Tevatron, to intermediate high-luminosity machines (the 3.6-TeV Tevatron upgrade or the 6-TeV UNK at Serpukhov), and on to future supercolliders LHC and SSC. Given the high likelihood that $b' \to bH$ is comparable to semileptonic $b' \to c,t$ decay or $b' \to bZ$, one would tag on the usual isolated high p_T lepton signal (heavy flavor or W boson production), or l^+l^- pairs that reconstruct to Z^0 bosons. The signal is rather similar to the usual $pp \to (WH \text{ or } ZH) + X$ processes. Direct WH and ZH production is not very promising,[3] since the cross section seems to be insufficient to overcome the QCD background for the typical Higgs-boson decay modes. However, in our case the production and decay process leading to the WH or ZH signal is quite different and separate. The b' quarks are pair produced via gluon fusion, and the strong cross section is much higher than the normal WH or ZH associated production. The b' pair subsequently decays, and due to a combination of mass thresholds and suppressed mixing angles, allow WH (W virtual or real) or ZH pairs to appear in the final state. For the subsequent Higgs-boson decay $H \to t\bar{t}$ is not likely to occur in our scenario, since one needs the top to be heavier than the Higgs boson. The decays $H \to WW, ZZ$ are possible when both b' and H are rather heavy, but a very heavy top quark is needed, while the same signal can be used to search for direct Higgs-boson production already. The signal, triple or even quadruple vector-boson production, will of course be quite spectacular. The Higgs boson is likely to decay into $b\bar{b}$ pairs within the scenario, given that $M_H > 20$ GeV or so already. The tagging of b quarks will be important, since the events may have up to six b-flavored hadrons in them. One could also look for the usual "rare" Higgs-boson decay modes[3] $H \to \tau^+\tau^-$, $H \to \gamma\gamma$, etc. Since the cross section for $gg \to b'\bar{b}' \to (\bar{c}W^*)(bH)$ or $(\bar{b}Z)(bH)$, if allowed, should be much larger than direct associated WH and ZH production, detailed background studies under this new scenario should be redone. We do not consider this matter further.

C. Discussion

We have pointed out that if a fourth-generation b' quark exists and is lighter than $m_t + M_W$, it may provide a useful hunting ground for Higgs bosons. As present limits on m_t are quite high, this gives a rather good coverage of the so-called "intermediate-mass Higgs-boson" region of $M_Z \lesssim M_H \lesssim 2M_W$, especially if the b' is rather heavy. We would like to compare our signature with similar ones that have been proposed in the literature so far.

Regarding ZH pair production, it has been pointed out that, again if a fourth generation exists, $gg \to \eta_{b'} \to ZH$ constitutes a very good signal for finding the Higgs boson even for the intermediate-mass Higgs-boson region.[34] The relative merits of this process and ours are as follows. First, quarkonium production should be an extremely small fraction of the total $b'\bar{b}'$ cross section; hence, our process should be dominant. Second, our ZH mass spectrum should be broad whereas in the $\eta_{b'}$ case it is theoretically very narrow. Whether this can survive the reconstruction of the Higgs boson, due to poor b tagging or τ energy-momentum reconstruction, is a separate issue. Third, our mechanism is more involved, depending on many parameters than the mere existence of a fourth generation. It is, nevertheless, still quite general. In contrast, the $\eta_{b'}$ decay mechanism is somewhat simpler and works also for b' masses above 200 GeV, if its lifetime is long enough to allow the quarkonium to form (i.e., a sufficiently heavy top and suppressed $V_{cb'}$ is still needed). In any case, these are quite independent mechanisms, and they provide at least complementary handles on the search for (intermediate-mass) Higgs bosons.

We have taken a rather conservative stand on heavy fermions, namely, a more or less sequential fourth generation. This is, nowadays, becoming unpopular following the neutrino counting results from the Z^0 resonance, which indicates only three light neutrino families. We remark that having a fourth family with a heavy neutrino is in no way unnatural,[35] although it probably should not be called "sequential" anymore. In the event that one takes the neutrino counting result very conservatively and rejects the possibility of having a fourth generation completely, the signatures of large FCNC $Q \to bH$ and/or $Q \to bZ$ decay branching ratios can readily be obtained if there exist certain more exotic, heavy fermions. For example, if there are fermions with nonstandard representation structures, where the left- and right-handed fermion representations have the same weak multiplet structure, such as doublets or singlets, one would have FCNC couplings induced even at the tree level after diagonalization of the complete, like-charged, fermion mass matrix. Unitarity of the 3×3 KM matrix is lost but at the same time the Higgs boson and/or the Z^0 boson could have nondiagonal couplings. The nondiagonal couplings involving heavier standard fermions are naturally more sizable, which are precisely the ones less constrained by lower-energy phenomenology. In this example, the so-called vectorlike quarks could have origins from E_6 type of grand unified theories, supposedly motivated by superstring models. The possibility is well known and has very recently been studied by del Aguila, Kane, and Quirós,[36] where they report rather similar signatures as the ones considered here, although coming from a completely different origin. These authors also state that the presence of large FCNC rates can be used to distinguish vec-

torlike from standard-model quarks. As we have illustrated, this is clearly not the case. We remark that once a Dirac type of direct mass term is possible there is no handle on what the mass scale (called M_D in Ref. 36) should be, and given that we have no indications of them so far, one is inclined to conclude that they lie beyond the weak SU(2)-symmetry-breaking scale of 246 GeV, if not much higher. Such terms appear because there is no chiral symmetry forbidding them as with standard chiral fermion representations. These possibilities serve to emphasize the point that, in general, FCNC decays of new heavy fermions may well be sizable. If an almost sequential fourth generation exists, its mass scale is almost certainly not much higher than the weak symmetry-breaking scale, and the phenomenology follows. In contrast, with vectorlike fermions, one is at the mercy of nature to decide what M_D should be.

Finally, there is the possibility that the Higgs sector may be more complicated than the minimal standard-model Higgs boson assumed here. With a more general Higgs sector, there could be light pseudoscalars[37] as well, and how to distinguish between scalar versus pseudoscalar Higgs bosons would pose a challenge. Pantaleone and Roy[38] have suggested that the heavy vector quarkonia $\psi_Q \to Z +$Higgs-boson decay process may help distinguish the parity of the Higgs bosons that are present. However, once there are several light Higgs bosons present, the analysis would be even much more complicated by multiple parameters, and is outside the scope of the present paper. The most interesting case would be the two-doublet Higgs sector of minimal supersymmetry, which is highly constrained, and we intend to return to it in a future publication.

V. CONCLUSION

We have studied the FCNC decay mode $b' \to bH$ as a possible source for Higgs-boson production in hadronic colliders. A scenario is assumed in which the fourth-generation b' quark is lighter than $m_t + M_W$. In that case it is found that this mode could be substantial or even dominant. Production of $b'\bar{b}'$ via gluon fusion in which one b' subsequently decays producing a Higgs-boson and the other producing an isolated charged lepton $l^{\pm}$ (CC decay), or lepton pair $l^+ l^-$ (FCNC decay), then occurs with a sizable rate and provides a means of extracting the Higgs-boson signal from hadronic backgrounds. This tag could be especially useful in the "intermediate-mass range" $M_Z < M_H < 2M_W$.

The scenario for FCNC b' decay dominance is considerably extended as compared to earlier works. A complete discussion of the possible phenomenology is complicated by the large number of presently unknown masses and 4×4 KM matrix elements. Some general features do emerge however. If $m_{b'} \gtrsim m_t + M_W$ the CC decays would dominate and the FCNC modes would then be difficult to observe. For $M_Z < m_{b'} < m_t + M_W$, and depending somewhat on $V_{cb'}/V_{tb'}$, the three decay modes, $b' \to cW$, $b' \to bZ$, and $b' \to bH$, could all be of the same order of magnitude. For $m_{b'} < M_Z$, $b' \to bH$ is the dominant FCNC decay mode and if the decay $b' \to b\gamma$ is observed then the limit $M_H > m_{b'} - m_b$ is immediately implied.

For certain specific choices of the unknown masses, anomalous thresholds were encountered. We suggest a means of removing them in case they should be found to occur in a physical process.

The potential phenomenology, opened up by the scheme we have examined, has been shown to be very rich and might prove a boon to future high-energy colliders for which the expected physics output appears, at the present time, rather uncertain.

APPENDIX A

The scalar integrals B_0 and C_0 used in the text are defined as

$$B_0(p^2;m_1^2,m_2^2) = \int \frac{d^n q}{i\pi^2} \frac{1}{(q^2+m_1^2)[(q+p)^2+m_2^2]} ,$$

$$C_0(p_1^2,p_2^2,p_5^2;m_1^2,m_2^2,m_3^2) = \int \frac{d^n q}{i\pi^2} \frac{1}{(q^2+m_1^2)[(q+p_1)^2+m_2^2][(q+p_1+p_2)^2+m_3^2]} ,$$

where $p_5 = p_1 + p_2$

In terms of these scalar integrals, the effective $b'bH$ coupling in Eq. (2.1) with $m_b = 0$ and internal virtual-quark mass m_i has the relatively simple form

$$h_R^i = -\tfrac{1}{2} B_0(q^2;M_W^2,M_W^2) - \frac{m_i^2}{2M_W^2}\left[\frac{q^2+2m_i^2+4M_W^2}{q^2+m_{b'}^2}\right] B_0(q^2;m_i^2,m_i^2)$$

$$+ \left[\frac{2q^2M_W^2+2m_i^2M_W^2+m_i^2M_H^2+4M_W^4}{2M_W^2(q^2+m_{b'}^2)}\right] B_0(q^2;M_W^2,M_W^2)$$

$$+ \left[\frac{2m_i^4+2m_i^2M_W^2-m_i^2m_{b'}^2-m_i^2M_H^2-4M_W^4+2M_W^2m_{b'}^2}{2M_W^2(q^2+m_{b'}^2)}\right] B_0(-m_{b'}^2;m_i^2,M_W^2)$$

$$+\frac{(m_i^2-2M_W^2)}{2M_W^2}\left[\frac{m_i^2B_0(0;m_i^2,m_i^2)-M_W^2B_0(0;M_W^2,M_W^2)}{m_i^2-m_W^2}\right]+\frac{m_i^2-2M_W^2}{2M_W^2}\,.$$

$$-\frac{m_i^2}{2M_W^2}\left[\frac{q^2M_W^2+2m_i^4+2m_i^2M_W^2-m_i^2m_{b'}^2-4M_W^4+2M_W^2m_{b'}^2}{q^2+m_{b'}^2}\right]C_0(q^2,-m_{b'}^2,0;m_i^2,m_i^2,M_W^2)$$

$$+\frac{1}{2M_W^2(q^2+m_{b'}^2)}(q^2m_i^2M_H^2+2q^2M_W^4-2q^2M_W^2m_{b'}^2-2m_i^4M_W^2-m_i^4M_H^2-2m_i^2M_W^4$$

$$+2m_i^2M_W^2m_{b'}^2+m_i^2M_W^2M_H^2+m_i^2m_{b'}^2M_H^2+4M_W^6-2M_W^2m_{b'}^4)C_0(-m_{b'}^2,q^2,0;m_i^2,M_W^2,M_W^2)\,. \tag{A1}$$

This result can be reduced to Eq. (3.1) in the text by using expressions for the limits of B_0 and C_0 given in Ref. 5. The expression for h_R^i is logarithmically divergent with the divergence contained entirely in the first term. The sum of all subsequent terms is overall finite.

APPENDIX B

The decay rate $H\to b'\bar{b}$ can be obtained using Eq. (2.1) in the text as

$$\Gamma(H\to b'\bar{b})=\frac{3g^2}{32\pi}\left[\frac{g^2}{32\pi^2}\right]^2|V_{tb}V_{tb'}|^2\left[1-\frac{m_{b'}^2+m_b^2}{M_H^2}\right]\times\frac{m_{b'}^2M_H}{M_W^2}|\bar{h}_R|^2\frac{2|\mathbf{p}_{b'}|}{M_H}\,, \tag{B1}$$

where

$$2|\mathbf{p}_{b'}|/M_H=[1-(m_{b'}-m_b)^2/M_H^2]^{1/2}\times[1-(m_{b'}+m_b)^2/M_H^2]^{1/2}$$

is a phase-space factor, and the bar in $\bar{h}_R$ indicates that one should take $q=p_{b'}+p_b$ when using Eq. (A1). The $H\to b\bar{b}$ rate is

$$\Gamma(H\to b\bar{b})=\frac{3g^2}{32\pi}\left[1-\frac{4m_b^2}{M_H^2}\right]\frac{m_b^2M_H}{M_W^2}\frac{2|\mathbf{p}_b|}{M_H}\,, \tag{B2}$$

where $2|\mathbf{p}_b|/M_H=(1-4m_b^2/M_H^2)^{1/2}$ is the corresponding, unsuppressed phase-space factor. Comparing the two rates one finds that the gain in the effective coupling from m_b to $m_{b'}$ and possible heavy internal quark enhancements of $\bar{h}_R$ is insufficient to overcome the loop factor and phase-space suppression, and the branching ratio for $H\to b'\bar{b}$ is never above the percent level, even if $H\to b\bar{b}$ is the dominant Higgs-boson decay mode.

[1] J. E. Pilcher, in Proceedings of the DPF Summer Study, Snowmass, Colorado, 1990 (unpublished); A. Buijs, in Proceedings of the SLAC Summer Institute on Particle Physics, Standford, California, 1990 (unpublished).

[2] *Proceedings of the ECFA Workshop on LEP 200,* Aachen, West Germany, 1986, edited by A. Böhm and W. Hoogland (CERN Report No. 87-08, Geneva, Switzerland, 1987).

[3] See, e.g., J. F. Gunion *et al., The Higgs Hunter's Guide* (Addison-Wesley, Reading, MA, 1990); R. Cahn, Rep. Prog. Phys. **52**, 389 (1989), and references therein.

[4] W. S. Hou and R. G. Stuart, Phys. Rev. Lett. **62**, 617 (1989).

[5] W. S. Hou and R. G. Stuart, Nucl. Phys. **B320**, 277 (1989).

[6] MARK II Collaboration, G. S. Abrams *et al.*, Phys. Rev. Lett. **63**, 2447 (1989).

[7] S. C. Eno, Ph.D. thesis, Rochester University, 1989.

[8] VENUS Collaboration, K. Abe *et al.*, Phys. Rev. Lett. **63**, 1776 (1989).

[9] AMY Collaboration, S. Eno *et al.*, Phys. Rev. Lett. **63**, 1910 (1989).

[10] TOPAZ Collaboration, I. Adachi *et al.*, Phys. Lett. B **229**, 427 (1989).

[11] OPAL Collaboration, M. Z. Akrawy *et al.*, Phys. Lett. B **236**, 364 (1990).

[12] ALEPH Collaboration, D. Decamp *et al.*, Phys. Lett. B **236**, 511 (1990).

[13] B. Haeri, A. Soni, and G. Eilam, Phys. Rev. Lett. **62**, 719 (1989).

[14] A. D. Linde, Pis'ma Zh. Eksp. Teor. Fiz. **23**, 73 (1976) [JETP Lett. **23**, 64 (1976)]; Phys. Lett. **62B**, 435 (1976); S. Weinberg, Phys. Rev. Lett. **36**, 294 (1976).

[15] R. S. Willey and H. L. Yu, Phys. Rev. D **26**, 3086 (1982); **26**, 3287 (1982).

[16] W. S. Hou and R. G. Stuart, Phys. Lett. B **233**, 485 (1989).

[17] G. Eilam, B. Haeri, and A. Soni, Phys. Rev. D **41**, 875 (1990).

[18] MARK II Collaboration, G. S. Abrams *et al.*, Phys. Rev. Lett. **63**, 2173 (1989); L3 Collaboration, B. Adeva *et al.*, Phys. Lett. B **231**, 509 (1989); ALEPH Collaboration, D. Decamp *et al.*, *ibid.* **231**, 519 (1989); OPAL Collaboration, M. Z. Akrawy *et al.*, *ibid.* **231**, 530 (1989); DELPHI Collaboration, P. Aarnio *et al.*, *ibid.* **231**, 539 (1989).

[19] CDF Collaboration, F. Abe *et al.*, Phys. Rev. Lett. **64**, 147 (1990); Phys. Rev. D **43**, 646 (1991).

[20] W. S. Hou and R. G. Stuart, Phys. Lett. B **226**, 122 (1989).

[21] G. Passarino and M. Veltman, Nucl. Phys. **B160**, 151 (1979).

[22] R. G. Stuart, Comput. Phys. Commun. **48**, 367 (1988).

[23] R. G. Stuart and A. Góngora-T., Comput. Phys. Commun. **56**, 337 (1990).

[24] I. Bigi, Yu. L. Dokshitser, V. Khoze, J. H. Kühn, and P.

Zerwas, Phys. Lett. B **181**, 157 (1986).
[25]B. Grządkowski and P. Krawczyk, Z. Phys. C **18**, 43 (1983).
[26]J. D. Bjorken and S. D. Drell, *Relativistic Quantum Fields* (McGraw-Hill, New York, 1965).
[27]R. J. Eden, P. V. Landshoff, D. I. Olive, and J. C. Polkinghorne, *The Analytic S-matrix* (Cambridge Univ. Press, Cambridge, England, 1966).
[28]C. Itzykson and J.-B. Zuber, *Quantum Field Theory* (McGraw-Hill, New York, 1980).
[29]G. 't Hooft and M. Veltman, Nucl. Phys. **B153**, 365 (1979).
[30]We use a broad range of t, b', and t' mass values for illustrative reasons, in particular, to exhibit the strong $m_{t'}$ dependence of the $b' \to bH$ decay rate. These values would sometimes be in conflict with experimental limits from electroweak radiative corrections. We note, however, the presence of other new physics may compensate for heavy-fermion effects, and one should keep an open mind regarding new heavy-fermion masses.
[31]W. S. Hou and R. G. Stuart, Nucl. Phys. **B349**, 91 (1991).
[32]Note that if $m_{b'}$ is above the tW^* threshold, $b' \to tW^*$ becomes non-negligible compared to $b' \to cW$ when r is very small, although the $b' \to t$ transition turns on rather slowly.
[33]B. Grządkowski, in *Weak Interactions and Neutrinos,* Proceedings of the Twelfth International Workshop, Ginosar, Israel, 1989, edited by P. Singer and G. Eilam [Nucl. Phys. B (Proc. Suppl.) **13** (1989)].
[34]V. Barger *et al.*, Phys. Rev. Lett. **57**, 1672 (1986); Phys. Rev. D **35**, 3366 (1987).
[35]See C. T. Hill and E. A. Paschos, Phys. Lett. B **241**, 96 (1990), for a possible scenario.
[36]F. del Aguila, G. L. Kane, and M. Quirós, Phys. Rev. Lett. **63**, 942 (1989); F. del Aguila *et al.*, Nucl. Phys. **B334**, 1 (1990).
[37]Charged Higgs bosons would be in a different context since we are considering mainly effective FCNC decays. However, with extra charged Higgs bosons, the loop-induced FCNC rates can be further enhanced even if they are much heavier than the W boson.
[38]J. Pantaleone and P. Roy, Phys. Rev. Lett. **64**, 264 (1990).